



HAL
open science

Development and pilot-scale validation of a fuzzy-logic control system for optimization of methane production in fixed-bed reactors

Gabriel Capson-Tojo, M. V. Ruano, Eric Latrille, Jean-Philippe Steyer

► **To cite this version:**

Gabriel Capson-Tojo, M. V. Ruano, Eric Latrille, Jean-Philippe Steyer. Development and pilot-scale validation of a fuzzy-logic control system for optimization of methane production in fixed-bed reactors. *Journal of Process Control*, 2018, 68, pp.96-104. 10.1016/j.jprocont.2018.05.007 . hal-04182261

HAL Id: hal-04182261

<https://hal.inrae.fr/hal-04182261v1>

Submitted on 17 Aug 2023

HAL is a multi-disciplinary open access archive for the deposit and dissemination of scientific research documents, whether they are published or not. The documents may come from teaching and research institutions in France or abroad, or from public or private research centers.

L'archive ouverte pluridisciplinaire **HAL**, est destinée au dépôt et à la diffusion de documents scientifiques de niveau recherche, publiés ou non, émanant des établissements d'enseignement et de recherche français ou étrangers, des laboratoires publics ou privés.

Manuscript Number:

Title: Development and pilot-scale validation of a fuzzy-logic control system for optimization of methane production in fixed-bed reactors

Article Type: Research Paper

Keywords: Anaerobic digestion, bio-methane, fixed-bed reactor, fuzzy-logic control, optimization, winery wastewater

Corresponding Author: Dr. Angel Robles, Ph.D.

Corresponding Author's Institution: Universitat Politècnica de València

First Author: Angel Robles, Ph.D.

Order of Authors: Angel Robles, Ph.D.; Gabriel Capson-Tojo, M.Sc.; María Victoria Ruano, Ph.D.; Eric Latrille, Ph.D.; Jean-Philippe Steyer, Ph.D.

Abstract: The objective of this study was to develop an advanced control system for optimizing the performance of fixed-bed anaerobic reactors. The controller aimed at maximizing the bio-methane production whilst controlling the volatile fatty acids content in the effluent. For this purpose, a fuzzy-logic controller was developed, tuned and validated in an anaerobic fixed-bed reactor at pilot scale (350 litres) treating raw winery wastewater. The results showed that the controller was able to adequately optimize the process performance, maximizing the methane production, with an average methane yield of about 0.29 LCH₄ g⁻¹ COD. On the other hand, the controller maintained the volatile fatty acids content in the effluent close to the established maximum limit (750 mg COD L⁻¹). The outcomes of this study are expected to facilitate plant engineers to establish an optimal control strategy that enables an adequate process performance with the maximum bio-methane productivity.

Dear Editor,

Attached you will find the manuscript entitled “**Development and pilot-scale validation of a fuzzy-logic control system for optimization of methane production in fixed-bed reactors**” submitted for consideration as a research paper in Journal of Process Control. All the authors mutually agree for submitting this manuscript to Journal of Process Control. We confirm that it is the original work and that the work presented has not been submitted earlier to this Journal.

The main objective of this work was to develop an advanced control system for optimizing the performance of fixed-bed anaerobic reactors. The controller aimed at maximizing the bio-methane production whilst controlling the volatile fatty acids content in the effluent. To this aim, a fuzzy-logic controller was developed, tuned and validated in an anaerobic fixed-bed reactor at pilot scale treating raw winery wastewater. The outcomes of this study are expected to facilitate plant engineers to establish an optimal control strategy that enables an adequate process performance with the maximum bio-methane productivity.

The important findings that must be highlighted are:

- Simulation results show that the proposed controller is capable to achieve great process performances even when operating at high VFA concentrations.
- The controller was sufficient to capture the dynamics of the process around the corresponding set point.
- Pilot results showed the potential of this control approach to maintain the process working properly under similar conditions to the ones expected at full-scale plants.

Yours sincerely,

Ángel Robles Martínez, PhD

CALAGUA – Unidad Mixta UV-UPV

Departament d'Enginyeria Química, ETSE-UV.

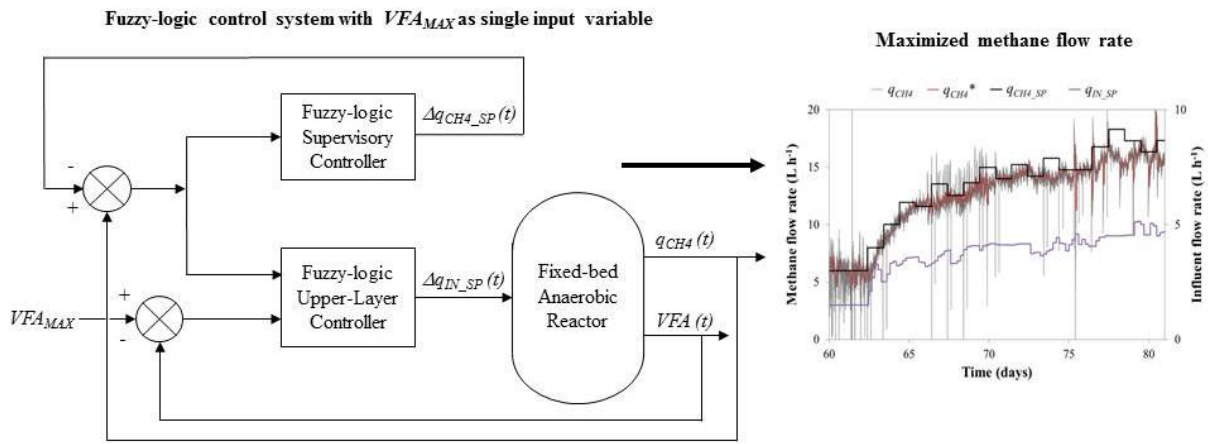
Universitat de València

Avinguda de la Universitat s/n, 46100, Burjassot, València, Spain

Tel.: +34 96 354 30 85

E-mail: angel.robles@uv.es

1 **Graphical abstract**



1 **Highlights**

- 2 • A fuzzy-logic control system for optimizing the methane production was proposed
- 3 • The controller was developed, tuned and validated at a 350 L pilot-scale system
- 4 • The controller aimed to maximize methane production whilst controlling VFA
- 5 contents
- 6 • Methane yields up to 0.29 L CH₄ g⁻¹ COD were achieved when running the
- 7 controller

1 **Development and pilot-scale validation of a fuzzy-logic control**
2 **system for optimization of methane production in fixed-bed reactors**

3 A. Robles^{a,b,*,**}, G. Capson-Tojo^b, M.V. Ruano^c, E. Latrille^b and J.-P. Steyer^b

4
5 ^a CALAGUA – Unidad Mixta UV-UPV, Institut Universitari d'Investigació
6 d'Enginyeria de l'Aigua i Medi Ambient – IIAMA, Universitat Politècnica de
7 València, Camí de Vera s/n, 46022, València, Spain. (E-mail: *ngelibma@upv.es*)

8 ^b LBE, INRA, 102 avenue des Etangs, 11100, Narbonne, France. (E-mail:
9 *gabriel.capson-tojo@supagro.inra.fr; eric.latrille@inra.fr; jean-*
10 *philippe.steyer@inra.fr*)

11 ^c CALAGUA – Unidad Mixta UV-UPV, Departament d'Enginyeria Química, ETSE-
12 UV, Universitat de València, Avinguda de la Universitat s/n, 46100, Burjassot,
13 València, Spain. (E-mail: *m.victoria.ruano@uv.es*)

14 * Corresponding author: Tel.: +34 96 354 30 85; E-mail: *angel.robles@uv.es*

15 ** *Current address: CALAGUA – Unidad Mixta UV-UPV, Departament*
16 *d'Enginyeria Química, ETSE-UV, Universitat de València, Avinguda de la*
17 *Universitat s/n, 46100, Burjassot, València, Spain. (E-mail: *angel.robles@uv.es*)*

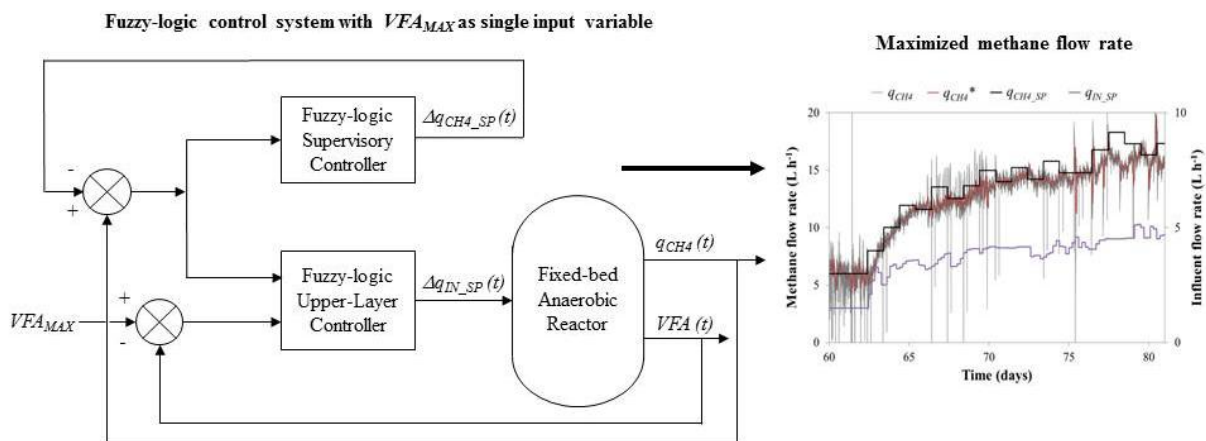
18
19 **Abstract**

20 The objective of this study was to develop an advanced control system for optimizing
21 the performance of fixed-bed anaerobic reactors. The controller aimed at maximizing
22 the bio-methane production whilst controlling the volatile fatty acids content in the
23 effluent. For this purpose, a fuzzy-logic controller was developed, tuned and
24 validated in an anaerobic fixed-bed reactor at pilot scale (350 litres) treating raw

25 winery wastewater. The results showed that the controller was able to adequately
 26 optimize the process performance, maximizing the methane production, with an
 27 average methane yield of about $0.29 \text{ L}_{\text{CH}_4} \text{ g}^{-1} \text{ COD}$. On the other hand, the controller
 28 maintained the volatile fatty acids content in the effluent close to the established
 29 maximum limit ($750 \text{ mg COD L}^{-1}$). The outcomes of this study are expected to
 30 facilitate plant engineers to establish an optimal control strategy that enables an
 31 adequate process performance with the maximum bio-methane productivity.

32

33 **Graphical abstract**



34

35 **Keywords**

36 Anaerobic digestion, bio-methane, fixed-bed reactor, fuzzy-logic control,
 37 optimization, winery wastewater

38

39 **Highlights**

- 40 • A fuzzy-logic control system for optimizing the methane production was proposed
- 41 • The controller was developed, tuned and validated at a 350 L pilot-scale system
- 42 • The controller aimed to maximize methane production whilst controlling VFA
- 43 contents

- 44 • Methane yields up to 0.29 L CH₄ g⁻¹ COD were achieved when running the
45 controller

46

47 **1. Introduction**

48

49 Nowadays, a major issue to overcome in order to achieve a global sustainable
50 development is our dependency on fossil fuels for electricity production, which represents up
51 to 80 % of the global energy consumption [1]. Therefore, one of the main challenges of this
52 century is to develop new competitive sources of renewable energy, capable of replacing
53 fossil fuels with a minimum impact on both environment and society [2]. In this context,
54 alternative energy sources must be pursued [3]. Bio-methane production from anaerobic
55 digestion (AD) of waste represents a promising option that can be considered as carbon
56 neutral due to its net balance of greenhouse gases emissions.

57

58 Due to the high methane productivities that can be achieved by high-rate anaerobic
59 reactors, a huge effort is currently being put on the study of systems such as up-flow
60 anaerobic sludge blanket (UASB), expanded granular sludge blanket (EGSB), anaerobic
61 membrane bioreactor (AnMBR) or fixed-bed bioreactor [4]. In these reactors, the biomass is
62 self-immobilized, allowing uncoupling the hydraulic retention time (HRT) and the solid
63 retention time (SRT).

64

65 However, the complexity and the diversity of the phenomena occurring in high-rate
66 anaerobic reactors have delayed the understanding, and consequently the proper control, of
67 this AD process. Due to the large number of factors that affect anaerobic processes, the
68 selection of proper monitoring indicators and the development of advanced control systems

69 are crucial for a successful optimization of the process performance [5,6].

70

71 Biogas composition and production rate are the most commonly used variables acting as
72 indicators of the process performance during AD. In addition, the methane yield (Y_{CH_4}),
73 which is usually defined as the amount of methane produced per unit of organic matter
74 removed, is also used as an indirect parameter for evaluating the performance of anaerobic
75 processes [7,8]. Nevertheless, these indicators can be insufficient to evaluate the overall
76 process performance. This is because they usually indicate too late disturbances affecting the
77 process, when there is no possible action to recover it immediately. To avoid this issue, the
78 concentration of volatile fatty acids (VFA) has been proved to be an adequate state indicator
79 for monitoring AD processes [9]. VFAs are main intermediate metabolites in AD and
80 therefore, monitoring their concentration can be a useful tool for process diagnosis (*e.g.* to
81 detect AD imbalances). Moreover, as this variable can be easily on-line monitored, for
82 instance by means of titrimetric sensors, it gives a much faster and more reliable information
83 than other common indicators applied for AD monitoring, such as pH, alkalinity, gas
84 composition or gas production [10–14].

85

86 Many different alternatives, such as classical Proportional-Integral-Derivative (PID)
87 control, fuzzy systems, neuron networks or model-based systems, have been applied for
88 controlling AD process [15]. Among these strategies, fuzzy-logic control has the main
89 advantage of being applicable to control non-linear systems, such as AD. A fuzzy-logic
90 controller [16] is able to optimize different types of processes under dynamic conditions by
91 applying valuable expert knowledge [17–20]. Moreover, fuzzy-logic controllers do not
92 require large amounts of data and/or rigorous mathematical models, thus allowing a much
93 simpler calibration of the controller. In addition, these control systems allow the development

94 of multiple-input-multiple-output control schemes. Hence, it can be stated that fuzzy logic is a
95 powerful tool for controlling anaerobic fixed-film reactors [21]. Therefore, fuzzy-logic
96 control has been widely implemented in wastewater treatment over the last decades and has
97 been successfully featured in several AD applications [22–26]. As listed in Jimenez et al. [15],
98 different applications of fuzzy-logic control systems for AD control can be found in the
99 literature. Taking some examples, Puñal et al [27] developed a PI-based fuzzy-logic controller
100 which used the dilution rate as manipulated variable to control the concentration of VFAs in
101 the effluent. In addition, Murnleitner et al. [28] applied fuzzy theory to avoid overloading of
102 AD reactors. Recently, Robles et al. [29] demonstrated the suitability of fuzzy-logic systems
103 for controlling the methane production in AD reactors using the methane flow rate and the
104 VFA concentration as input variables. Nevertheless, only one study has been carried out so far
105 for optimization of AD processes using fuzzy logic. Carlos-Hernandez et al. [30] proposed a
106 fuzzy supervisory controller to optimize the AD performance by controlling alkali addition
107 and the dilution rate. To the knowledge of the authors, no other study has been carried out to
108 apply fuzzy-logic control systems for AD optimization.

109

110 Considering the aforementioned information, the main objective of this study was to
111 develop an advanced control system for optimizing the methane production in fixed-bed
112 anaerobic reactors. To this purpose, a fuzzy-logic system consisting of a supervisory
113 controller to determine the set-point of methane flow rate and an upper-layer controller to
114 define the inflow of substrate into the reactor was first developed by simulation and then
115 validated in a 350 L pilot-scale fixed-bed anaerobic reactor treating industrial winery
116 wastewater. The proposed controller aimed at maximizing bio-methane production whilst
117 controlling the VFA concentration in the effluent. The main novelty of this study lies not only
118 in developing a controller for optimizing the operation of fixed-bed anaerobic reactors, but

119 also in its validation under specific conditions that were similar to those found in full-scale
120 plants.

121

122 **2. Materials and methods**

123

124 *2.1. Pilot plant description and operation*

125

126 Figure 1 shows the flow diagram and the instrumentation of the continuous fixed-bed
127 anaerobic reactor used in this study. The plant had a total volume of 358 L. The support media
128 (Cloisonyl: $180 \text{ m}^2 \text{ m}^{-3}$ specific surface) filled 34 L, leaving 324 L as effective volume. The
129 anaerobic reactor was jacketed and connected to a water heating system for temperature
130 control. Moreover, the plant was equipped with a pH control by feeding NaOH (30 %) to the
131 system when necessary. The pH set-point was set at 7.2.

132

133 The plant was fed with industrial winery wastewater from local cellars located in the area
134 of Narbonne, France. Table 1 shows the main average characteristics of the influent
135 wastewater during the experimental period. The wastewater was stored in a feeding tank of 27
136 m^3 that was connected to a dilution system of 0.2 m^3 . The main aim of this dilution system
137 was to allow testing different organic loading rates (OLRs) in the plant. In the reactor, a
138 portion of the mixed liquor was recycled from the bottom to the top for both improving the
139 mixing conditions and favouring the stripping of the produced gases from the liquid phase.
140 The influent wastewater was mixed with the recycled mixed liquor and then introduced at the
141 top of the reactor. The recycling flow rate was controlled manually at approximately 550 L h^{-1} .
142 ¹. The pilot plant was operated at a controlled temperature of $35 \text{ }^\circ\text{C}$.

143

144 2.2. Pilot plant instrumentation, automation and control

145

146 As shown in Figure 1, the plant was fully automated and instrumented. The on-line
147 equipment consisted of: one pH transmitter and one conductivity-temperature transmitter
148 located in the recycling pipe; one temperature transmitter in the anaerobic reactor; one gas
149 pressure transmitter in the head-space of the anaerobic reactor; two flow-rate transmitters (one
150 for the recycling pump and one for the feed pump); one gas flow-rate transmitter
151 (electromagnetic floater-based sensor) and one on-line CH₄/CO₂ sensor (Ultramat 22P
152 Siemens), both located in the biogas discharge pipeline; and one on-line titrimetric sensor
153 (Anaerobic Control Analyser AnaSense[®], AppliTek S.L.) for the measurement of total VFA
154 and alkalinity in the reactor. On the other hand, a linear relationship (R^2 above 0.8) was
155 observed between the experimentally determined COD concentration in the effluent and the
156 VFA measurement from the on-line titrimetric sensor. Therefore, besides its experimental
157 determination, the COD concentration in the effluent was also predicted in real time from the
158 continuously on-line monitored VFA concentration.

159

160 The plant also included several lower-layer control loops, which consisted of classical
161 PIDs and on-off controllers, in order to control the influent flow rate, the temperature, and the
162 pH. The on-line sensors and the automatic equipment were connected to a network system
163 that included several transmitters, an input/output device, and a PC that was in charge of the
164 data acquisition and allowed performing multi-parameter control. The input/output device was
165 managed by a software developed at INRA-LBE. The main aim of this software was to carry
166 out data logging, advanced control action calculations and process supervision by using
167 Matlab[®] routines.

168

169 *2.3. Sampling and off-line measurements*

170

171 Besides the on-line process monitoring, samples from influent, effluent and biogas
172 streams were collected once per day. From both influent and effluent, the chemical oxygen
173 demand (COD) was determined twice/three times a week, whilst the composition of VFAs,
174 *i.e.* acetate (C2), propionate (C3), iso-butyrate and butyrate (iC4 and C4), and iso-valerate and
175 valerate (iC5 and C5), were analyzed once per day. Biogas composition (CH₄, CO₂, O₂, H₂S,
176 and N₂) was determined three times a week.

177

178 The COD was determined by the spectrophotometric micro-method (Tube Test MR,
179 AQUALYTIC[®]), according to Standard Methods [31]. The composition of VFAs was
180 determined by liquid chromatography (Perkin Elmer[®], Clarus 580 Liquid Chromatograph).
181 0.5 mL of sample was introduced into a vial with the same amount of standard (1 g of ethyl-2-
182 butiric acid in 1 L of distilled water, acidified to 5 % (v/v) with H₃PO₄). Moreover, a control
183 solution containing the VFAs to be determined (1.078 g C2 L⁻¹; 1.022 g C3 L⁻¹; 1.068 g iC4
184 L⁻¹; 1.111 g C4 L⁻¹; 1.079 g iC5 L⁻¹; and 1.151 g C5 L⁻¹) was also analysed. The composition
185 of gas was measured using a gas chromatograph equipped with a thermic conductivity
186 detector (GC-TCD, Perkin Elmer[®], Clarus 480 Gas Chromatograph). 0.2 mL of biogas were
187 collected by a gas-tight syringe and injected into the GC, which was maintained at
188 temperature of 65 °C and pressure of 2.48 bars. The GC consisted of two columns: one
189 RtUBond (30m x 0.32mm x 10µm) allowing the separation of CO₂ and H₂S; and one Rt-
190 Molvieve 5A (30m x 0.32mm x 30µm) allowing the separation of the H₂, O₂, N₂ and CH₄.
191 The carrier gas was helium at a flow-rate of 4 mL min⁻¹.

192

193 *2.4. Control system description*

194

195 Figure 2 shows a block diagram of the proposed fuzzy-logic controller for optimization
196 of the performance of a fixed-bed anaerobic reactor. For that purpose the controller aimed at
197 maximizing the bio-methane production whilst controlling the VFA content in the effluent.
198 The proposed control structure consisted of: (i) an upper-layer controller that manipulated the
199 influent liquid flow to maintain the methane gas flow rate close to a given set-point; and (ii) a
200 supervisory controller that maximized the set-point of the methane flow rate to be controlled
201 by the upper-layer controller.

202

203 The methane flow was calculated by means of the methane concentration in the gas
204 phase and the measured biogas flow. The methane flow was corrected to account for the
205 dependence of the biogas density on the volumetric flow. Thus, taking into account the on-
206 line information from the biogas composition (% CH₄ and % CO₂) and the measured biogas
207 flow ($G_{MEASURED}$), the methane flow (q_{CH_4}) was calculated by Equation 1.

208

$$209 \quad q_{CH_4} = G_{CORRECTED} \cdot \frac{\%CH_4}{100} \quad (\text{Eq. 1})$$

210 where:

$$211 \quad - \quad G_{CORRECTED} = G_{MEASURED} \cdot frho \quad (\text{Eq. 2})$$

$$212 \quad - \quad frho = \sqrt{\frac{rho_{AIR}}{(rho_{CH_4} \cdot \%CH_4 + rho_{CO_2} \cdot \%CO_2 + rho_{N_2} \cdot (100 - \%CH_4 - \%CO_2)) / 100}} \quad (\text{Eq. 3})$$

213 - rho_{AIR} : volumetric weight of air (1.2930 kg m⁻³),

214 - rho_{CH_4} : volumetric weight of CH₄ (0.7168 kg m⁻³),

215 - rho_{CO_2} : volumetric weight of CO₂ (1.9768 kg m⁻³),

216 - rho_{N_2} : volumetric weight of N₂ (1.2505 kg m⁻³).

217

218 A 2h-moving average value for q_{CH_4} ($q_{CH_4}^*$) was applied to the raw data to reduce the
219 noise from the measurements. Similarly, a 2h-moving average value (VFA^*) was also
220 considered for the effluent VFA concentration to take into account the sampling time of the
221 on-line titrimetric sensor. Both moving average values were also selected on the basis of AD
222 process dynamics through experimental observations. The control time of the upper-layer
223 controller was set to 5 h and the control time of the supervisory controller was set to 24 h. The
224 fuzzy-logic controller was defined following the Takagi-Sugeno structure.

225

226 2.4.1. Upper-layer controller description

227

228 The upper-layer controller determined the variation in the set-point of the influent flow
229 rate (Δq_{IN_SP}) to be applied to the corresponding PID controller on the basis of three inputs:
230 the error in the methane flow rate (eq_{CH_4} ; Equation 4), the variation in the error of the
231 methane flow rate (Δeq_{CH_4} ; Equation 5) and the difference between a maximum VFA
232 concentration (VFA_{MAX}) and the VFA content in the effluent ($dVFA$; Equation 6).

233

$$234 \quad eq_{CH_4}(t) = q_{CH_4}(t) - q_{CH_4_SP}(t) \quad (\text{Eq. 4})$$

235 where:

236 - $eq_{CH_4}(t)$: error in the methane flow rate at a given time t ,

237 - $q_{CH_4}(t)$: measured methane flow rate at a given time t ,

238 - $q_{CH_4_SP}(t)$: methane flow rate set-point at a given time t .

239

240 $\Delta eq_{CH_4}(t) = |eq_{CH_4}(t)| - \delta \cdot |eq_{CH_4}(t-1)|$ (Eq. 5)

241 where:

242 - $\Delta eq_{CH_4}(t)$: variation in the error of the methane flow rate at a given time t ,

243 - $|eq_{CH_4}(t)|$: absolute value of the error in the methane flow rate at a given time t ,

244 - δ : modifying algebraic factor (Equation 7),

245 - $|eq_{CH_4}(t-1)|$: absolute value of the error in the methane flow rate at the previous

246 control action.

247

248 $dVFA(t) = VFA_{MAX} - VFA(t)$ (Eq. 6)

249 where:

250 - $dVFA(t)$: difference between VFA_{MAX} and the VFA content in the effluent at a given
251 time t ,

252 - $VFA(t)$: effluent VFA concentration at a given time t ,

253 - VFA_{MAX} : maximum effluent VFA concentration.

254

255 Δeq_{CH_4} is negative or positive depending on whether $eq_{CH_4}(t)$ tends to zero or not,

256 respectively. Moreover, this equation features a modifying algebraic factor (δ) that is defined

257 by Equation 7 to account for opposite signs between $|eq_{CH_4}(t)|$ and $|eq_{CH_4}(t-1)|$.

258

259 $\delta = \frac{eq_{CH_4}(t) \cdot eq_{CH_4}(t-1)}{|eq_{CH_4}(t) \cdot eq_{CH_4}(t-1)|}$ (Eq. 7)

260

261 For the fuzzification stage, three Gaussian membership functions, represented by
 262 Equation 8, were considered for eq_{CH_4} and Δeq_{CH_4} : Negative (*N*), Zero (*Z*) and Positive (*P*);
 263 and one Gaussian membership function was defined for *dVFA*: Zero (*Z*). As each Gaussian
 264 membership function is defined by two parameters (centre *c* and amplitude *a*), the control
 265 system had a total of 14 parameters as regards to the fuzzification stage. Concerning the
 266 defuzzification stage, four singleton membership functions were defined for Δq_{IN_SP} : High
 267 Negative (*HN*), Low Negative (*LN*), Low Positive (*LP*) and High Positive (*HP*). Therefore,
 268 the control system had a total of 4 parameters regarding the defuzzification stage.

269

$$270 \quad \mu(p) = \exp\left(-\frac{(p-c)^2}{2\sigma^2}\right) \quad (\text{Eq. 8})$$

271 where:

- 272 - $\mu(p)$: degree of membership of the input variable *p*,
- 273 - *p*: numerical value of the variable,
- 274 - *c*: centre of the Gaussian-type membership function,
- 275 - σ : amplitude of the Gaussian-type membership function.

276

277 Table 2 shows the resulting grade of membership to the different output linguistic labels
 278 that define the output fuzzy set. As this table shows, the effect of the input variable *dVFA*
 279 (represented by the third right-side term of rules #1, #2, #5a and #6b, *i.e.* $1 - \mu(dVFA)_Z$) on
 280 the output linguistic variable decreases as the effluent VFA concentration decreases (*i.e.* if μ
 281 $(dVFA)_Z = 0$ then $1 - \mu(dVFA)_Z = 1$). On the contrary, the effect of *dVFA* cancels the
 282 corresponding control action when the effluent VFA concentration is close to VFA_{MAX} (*i.e.* if
 283 $\mu(dVFA)_Z = 1$ then $1 - \mu(dVFA)_Z = 0$). Hence, the increase in the influent flow rate

284 controlled by the inference rules #1, #2, #5a and #6b is cancelled when the system is working
285 at maximum VFA capacity.

286

287 The output linguistic variable (Δq_{IN_SP}) was obtained by applying Larsen's fuzzy
288 inference method [32]. In the defuzzification stage, the Height Defuzzifier method was
289 employed [33] to obtain a single output value from the output fuzzy set.

290

291 Finally, the control action of the upper-layer controller was calculated as expressed by
292 Equation 9.

293

$$294 \quad q_{IN_SP}(t) = q_{IN_SP}(t-1) + \Delta q_{IN_SP}(t) \quad (\text{Eq. 9})$$

295

296 2.4.2. Supervisory controller description

297

298 The supervisory controller determined the variation in the set-point of the methane flow
299 rate ($\Delta q_{CH_4_SP}$) on the basis of two inputs: the error in the methane flow rate (Equation 4) and
300 the accumulated error in the methane flow rate (Equation 10).

301

$$302 \quad \Sigma eq_{CH_4}(t) = \Sigma eq_{CH_4}(t-1) + ST \cdot eq_{CH_4}(t) \quad (\text{Eq. 10})$$

303 where:

- 304 - $\Sigma eq_{CH_4}(t)$: accumulated error in the methane flow rate at a given time,
- 305 - $\Sigma eq_{CH_4}(t-1)$: accumulated error in the methane flow rate at the previous sampling
306 time (ST),

307

308 Regarding the fuzzification stage, three additional Gaussian membership functions were
309 considered for Σeq_{CH_4} : Negative (*N*), Zero (*Z*) and Positive (*P*). Concerning the
310 defuzzification stage, three singleton membership functions were defined for $\Delta q_{CH_4_SP}$: Low
311 Negative (*LN*), Low Positive (*LP*) and High Positive (*HP*). Thus, the supervisory controller
312 added to the proposed fuzzy-logic controller a total of 6 and 3 parameters regarding
313 fuzzification and defuzzification, respectively. Table 2 shows the resulting grade of
314 membership to the different output linguistic labels that defined the output fuzzy set of the
315 supervisory controller.

316

317 The output linguistic variable ($\Delta q_{CH_4_SP}$) was determined following the method described
318 in section 2.4.2. Finally, the control action of the supervisory controller was calculated as
319 expressed by Equation 11.

320

$$321 \quad q_{CH_4_SP}(t) = q_{CH_4_SP}(t-1) + \Delta q_{CH_4_SP}(t) \quad (\text{Eq. 11})$$

322

323 *2.4.3. Simulation-based design and validation*

324

325 The controller was firstly designed and tuned by simulation in Matlab[®] Simulink[®] using
326 the Fuzzy Logic Toolbox[™]. To this aim, a simplified version of the model BNRM2 [34] was
327 used. This model considers the main physicochemical and biological processes taking place
328 during AD, including gas-liquid transfer (nitrogen, ammonia, oxygen, hydrogen, methane and
329 carbon dioxide), a chemical model for pH calculation and biological steps such as
330 acidogenesis, acetogenesis and acetoclastic and hydrogenotrophic methanogenesis. Therefore,
331 this model allowed the simulation of the methane production rates and the concentrations of

332 VFAs in the effluent.

333

334 The control tuning was performed by a trial-error approach until obtaining an adequate
335 response (*i.e.* a deviation of less than 5 % between the response and the set-point given by the
336 supervisory controller).

337

338 **3. Results and discussion**

339

340 *3.1. Simulation-based validation of the control system*

341

342 Figure 3 shows the performance of the advanced controller obtained by simulation after
343 control tuning. Figure 3a presents the evolution of the resulting methane flow rate and the
344 corresponding set-point commanded by the supervisory controller, and the influent flow rate
345 commanded by the upper-layer controller. Figure 3b shows the effluent VFA concentration
346 and the VFA_{MAX} considered. VFA_{MAX} was set to 750 mg COD L⁻¹ (value fixed from knowledge
347 obtained from previous experiments). This maximum VFA concentration resulted in a
348 minimum COD removal efficiency of 80%.

349

350 It must be mentioned that the value of VFA_{MAX} has to be carefully selected according to
351 the control objectives (*i.e.* enhance AD performance and stability, minimize VFA contents in
352 the effluent, meet COD discharge limits, achieve VFA requirements in downstream
353 processes...) and process specificities. For instance, higher VFA_{MAX} values can be potentially
354 applied without risk of reactor acidification if the controller performs in a high-alkalinity
355 system. On the other hand, lower VFA_{MAX} values should be applied when the alkalinity of the
356 system is low or when no pH control is possible, thus reducing the propensity of possible

357 acidification problems.

358

359 As Figure 3a shows, the controller was able to maintain the simulated methane flow at
360 values close to the controlled set-point until reaching the constraint of the maximum VFA
361 concentration ($750 \text{ mg COD L}^{-1}$). This maximum VFA concentration was approached from
362 days 5 to 6, thus the increase in the influent flow rate was almost null. Only when the VFA
363 concentration was below its maximum threshold value it was possible to increase slightly the
364 influent flow rate to compensate the negative error in the methane flow (see period from day 6
365 to end). As the differences between the measured and the desired values were getting smaller,
366 also did the changes in $q_{CH_4_SP}$ and q_{IN_SP} . Within an infinite time and no external
367 disturbances, the concentrations of VFA would eventually reach VFA_{MAX} , showing an optimal
368 performance according to the desired VFA content in the effluent.

369

370 It is important to notice that during the first period of simulation, when the VFA
371 concentrations were low, the methane production was higher than the one commanded by the
372 supervisory controller (*e.g.* 2nd day). However, the supervisory controller did not increase
373 more the set-point in order to avoid overloading the reactor.

374

375 3.2. *Experimental validation of the control system*

376

377 Figure 4 presents the evolution of the OLR and HRT throughout the experimental period.
378 As it can be observed, the operational period is divided in 3 different sections: (I) reactor
379 start-up; (II) transitory period including a pH-shock due to failure of the pH sensor; and (III)
380 controlled process. As Figure 4 shows, the OLR was manually increased from 0 to 4 g COD
381 $\text{L}^{-1} \text{ d}^{-1}$ from day 0 to around 40, whilst maintaining the HRT around 3 d. This progressive

382 increase in the OLR was carried out to minimize possible disturbances during the biofilm
383 formation at the start-up process. During this period, the concentration of VFAs in the effluent
384 was used as state indicator of the process performance. This allowed avoiding the inhibition
385 of the newly-grown biomass due to overloading of the reactor. This is the reason for the
386 decrease in the OLR from days 20 to 30. During this period, high VFA concentrations were
387 observed in the effluent (up to 1500 mg COD L⁻¹) and, as the acetate inhibition coefficient of
388 propionic-oxidizing bacteria is around 2500 mg COD L⁻¹ (see, for instance, Siegert and Banks
389 [35]), the OLR was reduced to avoid inhibition of these microorganisms. Around day 50
390 (period II in Figure 4), a significant increase of the pH in the reactor (up to around 9) occurred
391 due to a failure in the lower-layer pH controller (data not shown). This resulted in a
392 considerable decay of the anaerobic biomass. Therefore, the OLR and HRT were set to 1.4 g
393 COD L⁻¹ d⁻¹ and 9 d, respectively, in order to recover the system to appropriate operating
394 conditions. From day 61 on (period III in Figure 4), the advanced controller was turned on for
395 optimizing the process performance. Figure 4 shows that the controller increased
396 progressively the inflow to the reactor until reaching the maximum treatment capacity of the
397 system, which was limited by VFA_{MAX} (set at 750 mg COD L⁻¹).

398

399 Figure 5 shows the evolution throughout the operational period of: the methane yield
400 (Figure 5a); and the total COD removed in the system and the COD fraction removed for
401 methane production (Figure 5b). As Figure 5 shows, no methane production was observed
402 until day 20. This suggests that the removal of COD from days 10 to 20 was mainly related to
403 the anabolism of the anaerobic biomass (*i.e.* initial growth, fixation, and acclimation of the
404 biomass [7]) and to the production of the gas required for filling the headspace volume of the
405 reactor and to achieve conditions of gas-liquid equilibrium within the system. Therefore, 20
406 days was identified in this study as the minimum time for obtaining a functional anaerobic

407 biomass consortium under conditions of equilibrium. The decrease in the COD removal
408 observed from days 25 to 30 was related to the aforementioned accumulation of VFAs. After
409 decreasing the OLR, the COD removal efficiency was restored. From day 30 to around 50, a
410 quite stable COD removal efficiency (up to 85 %) was achieved. Concerning to the methane
411 yields after day 20, this value increased greatly (reaching values up to 0.34 L_{CH₄} per gram of
412 COD removed) due to catabolism of methanogenic archaea. However, this value decreased
413 from 0.32 to 0.10 L_{CH₄} g⁻¹ COD_{REM} from day 25 to day 30. According to Michaud et al. [7],
414 this may have been caused by disturbances occurring during the initial contact of the
415 microorganisms and the fixed support media. Therefore, even it after 20 days a functional
416 anaerobic biomass existed, a minimum time of 35 days was needed to obtain a functional
417 anaerobic biofilm. This value is in agreement with previous results reported in the literature
418 (see, for instance, Michaud et al. [7]). Afterwards, the methane yield increased continuously
419 throughout this operational period (except for period II), reaching again values up to 0.34
420 L_{CH₄} g⁻¹ COD_{REM}. This behaviour suggested the development and maturing of a stable
421 biofilm.

422

423 As mentioned before, during period II a system failure occurred due to a pH-shock. As
424 Figure 5 illustrates, both COD removal for methane production and methane yield presented a
425 sharp decrease. Nevertheless, when the control system was turned back on (period III), it was
426 possible to quickly recover the system to the previous state, achieving values of methane
427 yields and COD removals for methane production of around 0.34 L_{CH₄} g⁻¹ COD_{REM} and 85 %,
428 respectively.

429

430 The fixed-bed anaerobic reactor achieved an efficient and stable performance when
431 running the proposed advanced controller (period III). As Figure 5b shows, COD removal

432 efficiencies above 80 % were achieved during this period. In addition, a high stable methane
433 yield of around $0.34 \text{ L}_{\text{CH}_4} \text{ g}^{-1} \text{ COD}_{\text{REM}}$ was reached (see Figure 5a). These results highlighted
434 the suitable performance of the process under controlled conditions. Indeed, comparing the
435 results from periods I and III, it can be stated that enhanced process performances were
436 achieved in terms of COD removal, methane production and treatment capacity.

437

438 Figure 6 shows the performance of the advanced controller during the operational period
439 III. As it can be observed, the supervisory controller increased continuously the set-point for
440 the methane flow rate (see Figure 6a) until reaching the maximum effluent VFA concentration
441 (see Figure 6b). Therefore, the upper-layer controller continuously increased the influent flow
442 to reach the corresponding methane flow rate set-point. As a result, a maximum methane
443 production of around 17 L h^{-1} was reached when operating with a VFA_{MAX} of $750 \text{ mg COD L}^{-1}$
444 ¹. A deviation of the methane flow rate from the established set-point lower than 10 % was
445 achieved, whilst the methane yield was maintained around $0.35 \text{ L}_{\text{CH}_4} \text{ g}^{-1} \text{ COD}$ during the
446 pseudo-stationary operational period (see days 65 to the end in Figure 5a). Throughout this
447 period, a methane-rich biogas was also produced (with methane contents in the biogas around
448 $85 \pm 2 \%$).

449

450 As designed, the controller increased $q_{\text{CH}_4_SP}$ only if the concentration of VFA in the
451 effluent was below VFA_{MAX} . The results from days 70 to 73 show that, even if eq_{CH_4} was
452 negative (*i.e.* $q_{\text{IN_SP}}$ could be higher), the supervisory controller did not allow increasing the
453 influent flow rate because the concentration of VFA was over VFA_{MAX} . The same occurred the
454 days 77-78, verifying the correct performance of the controller.

455

456 As explained in section 3.1., without disturbances the process would reach eventually
457 VFA_{MAX} , never overpassing it. However, this value was reached and overpassed in different
458 occasions, suggesting that, as in any real process, disturbances affected the system. As the
459 temperature and the pH were controlled and kept at barely constant values, the most likely
460 sources of disturbances were the feed itself and the recirculation flow. Heterogeneity of the
461 substrate may have caused small differences in the COD entering the reactor. In addition, as
462 the substrate was kept into a feeding tank before entering the reactor, some extent of
463 degradation had already occurred during the storage period, modifying the input concentration
464 of VFA. Moreover, as the recirculation flow was manually controlled, there were sudden
465 drops in the recycling flow rate due to partial clogging of the tubing. This caused significant
466 variations of this parameter throughout the operational period (varying from 100 to 700 L h⁻¹).
467 This may have affected the methane production, mainly by modifying the stripping rate of the
468 produced gases from the liquid phase. Lower recycling flow rates might cause lower methane
469 stripping rates from the liquid phase, leading to lower gaseous outflow rates of methane.
470 However, the control action was able to compensate the disturbances in the methane
471 production, achieving anyway the desired set-point. Therefore, the fuzzy-logic control action
472 resulted in a suitable performance under disturbances which are likely to be similar to those
473 expected in full-scale plants (*e.g.* variations in the recycling flow rate).

474

475 It can be concluded that, after a relatively simple calibration, the proposed fuzzy-logic
476 controller was able to successfully optimize the process performance, maximizing the
477 methane production and the VFA content in the effluent up to the chosen fixed values, whilst
478 resulting in adequate COD removal efficiencies and methane yields. At this point, it is
479 important to mention that, as the organic matter within the winery wastewater used as
480 substrate is mainly composed of soluble COD, the AD kinetics were not limited by the

481 hydrolysis step. This allowed the application of a short period for the evaluation of the control
482 strategy.

483

484 Finally, when considering the application of this fuzzy-logic control system at full-scale
485 for control and optimization, different modifications might be considered to further improve
486 the performance, such as optimization of the control dynamics for both controllers, fine
487 adjustment of the knowledge-based fixed values (*i.e.*, VFA_{MAX}) and optimization of the tuning
488 parameters (*i.e.* centre, amplitude and singleton values for the fuzzification and
489 defuzzification stages), among others.

490

491 **4. Conclusions**

492

493 A fuzzy-logic based controller for optimizing the process performance of a 350 L fixed-
494 bed anaerobic reactor treating winery wastewater was developed by simulation and validated
495 under specific conditions that were similar to the ones expected at full-scale plants. The
496 controller aimed at maximizing the methane productivity whilst controlling the VFA content
497 in the effluent. By application of the fuzzy-logic control system, a deviation of the methane
498 flow from the established set-point lower than 10 % was achieved. The methane yield resulted
499 in values around $0.29 \text{ L}_{\text{CH}_4} \text{ g}^{-1} \text{ COD}$, with COD removal efficiencies of up to 85 % obtained
500 throughout the whole experimental period. On the other hand, the controller allowed an
501 adequate control of the VFA content in the effluent, with values close to the established set-
502 point ($750 \text{ mg COD L}^{-1}$). Hence, the proposed fuzzy-logic controller was able to successfully
503 control the system performance close to optimal conditions, maximizing the methane
504 productivity and the VFA concentration, whilst resulting in adequate COD removal
505 efficiencies and methane yields.

506

507 **Acknowledgements**

508

509 This research work has been supported by the Spanish Research Foundation (MICINN
510 FPI grant BES-2009-023712), which is gratefully acknowledged.

511

512 **References**

513

514 [1] X.M. Guo, E. Trably, E. Latrille, H. Carrre, J.P. Steyer, Hydrogen production from
515 agricultural waste by dark fermentation: A review, *Int. J. Hydrogen Energy*. 35 (2010)
516 10660–10673.

517 [2] C.A. Aceves-Lara, E. Latrille, J.P. Steyer, Optimal control of hydrogen production in a
518 continuous anaerobic fermentation bioreactor, *Int. J. Hydrogen Energy*. 35 (2010)
519 10710–10718.

520 [3] I. Angelidaki, P. Kongjan, Biorefinery for sustainable biofuel production from energy
521 crops; conversion of lignocellulose to bioethanol, biohydrogen and methane, in: 11th
522 IWA World Congr. Anaerob. Dig., Brisbane, Australia, 2007.

523 [4] E. Aguilar-Garnica, D. Dochain, V. Alcaraz-González, V. González-Álvarez, A
524 multivariable control scheme in a two-stage anaerobic digestion system described by
525 partial differential equations, *J. Process Control*. 19 (2009) 1324–1332.

526 [5] J. Von Sachs, U. Meyer, P. Rys, H. Feitkenhauer, New approach to control the
527 methanogenic reactor of a two-phase anaerobic digestion system, *Water Res*. 37 (2003)
528 973–982.

529 [6] L. Lardon, A. Puñal, J.-P. Steyer, On-line diagnosis and uncertainty management using
530 evidence theory—experimental illustration to anaerobic digestion processes, *J. Process*

- 531 Control. 14 (2004) 747–763.
- 532 [7] S. Michaud, N. Bernet, P. Buffière, M. Roustan, R. Moletta, Methane yield as a
533 monitoring parameter for the start-up of anaerobic fixed film reactors, *Water Res.* 36
534 (2002) 1385–1391.
- 535 [8] A. Ghouali, T. Sari, J. Harmand, Maximizing biogas production from the anaerobic
536 digestion, *J. Process Control.* 36 (2015) 79–88.
- 537 [9] K. Boe, D.J. Batstone, J.-P. Steyer, I. Angelidaki, State indicators for monitoring the
538 anaerobic digestion process, *Water Res.* 44 (2010) 5973–5980.
539 <http://dx.doi.org/10.1016/j.watres.2010.07.043>.
- 540 [10] J.P. Steyer, J.C. Bouvier, T. Conte, P. Gras, J. Harmand, J.P. Delgenes, On-line
541 measurements of COD, TOC, VFA, total and partial alkalinity in anaerobic digestion
542 processes using infra-red spectrometry, *Water Sci. Technol.* 45 (2002) 133–138.
- 543 [11] J.P. Steyer, J.C. Bouvier, T. Conte, P. Gras, P. Sousbie, Evaluation of a four year
544 experience with a fully instrumented anaerobic digestion process, *Water Sci. Technol.*
545 45 (2002) 495–502.
- 546 [12] C. Charnier, E. Latrille, L. Lardon, J. Miroux, J.P. Steyer, Combining pH and electrical
547 conductivity measurements to improve titrimetric methods to determine ammonia
548 nitrogen, volatile fatty acids and inorganic carbon concentrations, *Water Res.* 95 (2016)
549 268–279.
- 550 [13] A.D. Kalafatis, L. Wang, W.R. Cluett, Linearizing feedforward-feedback control of pH
551 processes based on the Wiener model, *J. Process Control.* 15 (2005) 103–112.
- 552 [14] A. Schaum, J. Alvarez, J.P. Garcia-Sandoval, V.M. Gonzalez-Alvarez, On the
553 dynamics and control of a class of continuous digesters, *J. Process Control.* 34 (2015)
554 82–96.
- 555 [15] J. Jimenez, E. Latrille, J. Harmand, A. Robles, J. Ferrer, D. Gaida, C. Wolf, F. Mairet,

- 556 O. Bernard, V. Alcaraz-Gonzalez, Instrumentation and control of anaerobic digestion
557 processes: a review and some research challenges, *Rev. Environ. Sci. Bio/Technology*.
558 14 (2015) 615–648.
- 559 [16] L.A. Zadeh, Fuzzy sets, *Inf. Control*. 8 (1965) 338–353.
- 560 [17] H.B. Verbruggen, P.M. Bruijn, Fuzzy control and conventional control: What is (and
561 can be) the real contribution of Fuzzy Systems?, *Fuzzy Sets Syst.* 90 (1997) 151–160.
- 562 [18] M. V Ruano, J. Ribes, G. Sin, A. Seco, J. Ferrer, A systematic approach for fine-tuning
563 of fuzzy controllers applied to WWTPs, *Environ. Model. Softw.* 25 (2010) 670–676.
- 564 [19] A. Robles, M.V. Ruano, J. Ribes, J. Ferrer, Advanced control system for optimal
565 filtration in submerged anaerobic MBRs (SAnMBRs), *J. Memb. Sci.* 430 (2013) 330–
566 341.
- 567 [20] A. Robles, M. V Ruano, J. Ribes, A. Seco, J. Ferrer, Model-based automatic tuning of a
568 filtration control system for submerged anaerobic membrane bioreactors (AnMBR), *J.*
569 *Memb. Sci.* 465 (2014) 14–26.
- 570 [21] G. Olsson, M.K. Nielsen, Z. Yuan, A. Lynggaard-Jensen, Instrumentation, control and
571 automation in wastewater systems, IWA publishing, 2005.
- 572 [22] M. Estaben, M. Polit, J.P. Steyer, Fuzzy control for an anaerobic digester, *Control Eng.*
573 *Pract.* 5 (1997) 1303–1310.
- 574 [23] A. Genovesi, J. Harmand, J.P. Steyer, A fuzzy logic based diagnosis system for the on-
575 line supervision of an anaerobic digester pilot-plant, *Biochem. Eng. J.* 3 (1999) 171–
576 183.
- 577 [24] O. Bernard, M. Polit, Z. Hadj-Sadok, M. Pengov, D. Dochain, M. Estaben, P. Labat,
578 Advanced monitoring and control of anaerobic wastewater treatment plants: software
579 sensors and controllers for an anaerobic digester, *Water Sci. Technol.* 43 (2001) 175–
580 182.

- 581 [25] M. Polit, A. Genovesi, B. Claudet, Fuzzy logic observers for a biological wastewater
582 treatment process, *Appl Numer Math.* 39 (2001) 173–180.
- 583 [26] Á. Robles, F. Durán, M.V. Ruano, J. Ribes, A. Rosado, A. Seco, J. Ferrer,
584 Instrumentation, control, and automation for submerged anaerobic membrane
585 bioreactors, *Environ. Technol.* 36 (2015) 1–12.
- 586 [27] A. Puñal, L. Palazzotto, J.C. Bouvier, T. Conte, J.P. Steyer, Automatic control of
587 volatile fatty acids in anaerobic digestion using a fuzzy logic based approach, *Water*
588 *Sci. Technol.* 48 (2003) 103–110.
- 589 [28] E. Murnleitner, T.M. Becker, A. Delgado, State detection and control of overloads in
590 the anaerobic wastewater treatment using fuzzy logic, *Water Res.* 36 (2002) 201–211.
- 591 [29] A. Robles, E. Latrille, M. V. Ruano, J.P. Steyer, A fuzzy-logic-based controller for
592 methane production in anaerobic fixed-film reactors, *Environ. Technol.* 38 (2017).
- 593 [30] S. Carlos-Hernandez, J.F. Beteau, E.N. Sanchez, Intelligent control strategy for an
594 anaerobic fluidized bed reactor, *IFAC Proc. Vol.* 40 (2007) 73–78.
- 595 [31] APHA, *Standard Methods for the Examination of Water and Wastewater*, 21st ed.,
596 American Public Health Association, Washington, DC, 2005.
- 597 [32] P.M. Larsen, Industrial applications of fuzzy logic control, *Int. J. Man. Mach. Stud.* 12
598 (1980) 3–10.
- 599 [33] J.M. Mendel, Fuzzy logic systems for engineering: a tutorial, *Proc. IEEE.* 83 (1995)
600 345–377.
- 601 [34] R. Barat, J. Serralta, M. V Ruano, E. Jiménez, J. Ribes, A. Seco, J. Ferrer, Biological
602 Nutrient Removal Model No. 2 (BNRM2): a general model for wastewater treatment
603 plants, *Water Sci. Technol.* 67 (2013) 1481–1489.
- 604 [35] I. Siegert, C. Banks, The effect of volatile fatty acid additions on the anaerobic
605 digestion of cellulose and glucose in batch reactors, *Process Biochem.* 40 (2005) 3412–

606 3418.

607

608 **Figure and table captions**

609 **Figure 1.** Flow diagram of the plant, including instrumentation. (Nomenclature: **FIT**: Flow-
610 Indicator-Transmitter; **PIT**: Pressure-Indicator-Transmitter; **pH**: pH-Transmitter; **CT**:
611 Conductivity-Transmitter; **T**: Temperature sensor; **PLC**: Programmable Logic Controller).

612 **Figure 2.** Flow diagram of the advanced fuzzy-logic controller

613 **Figure 3.** Simulation of the control system performance. Evolution of: **(a)** methane flow and
614 influent flow; and **(b)** VFA content in the effluent

615 **Figure 4.** Evolution during the operational period of OLR and HRT. (I), (II) and (III) stand
616 for the different sections of the operational period

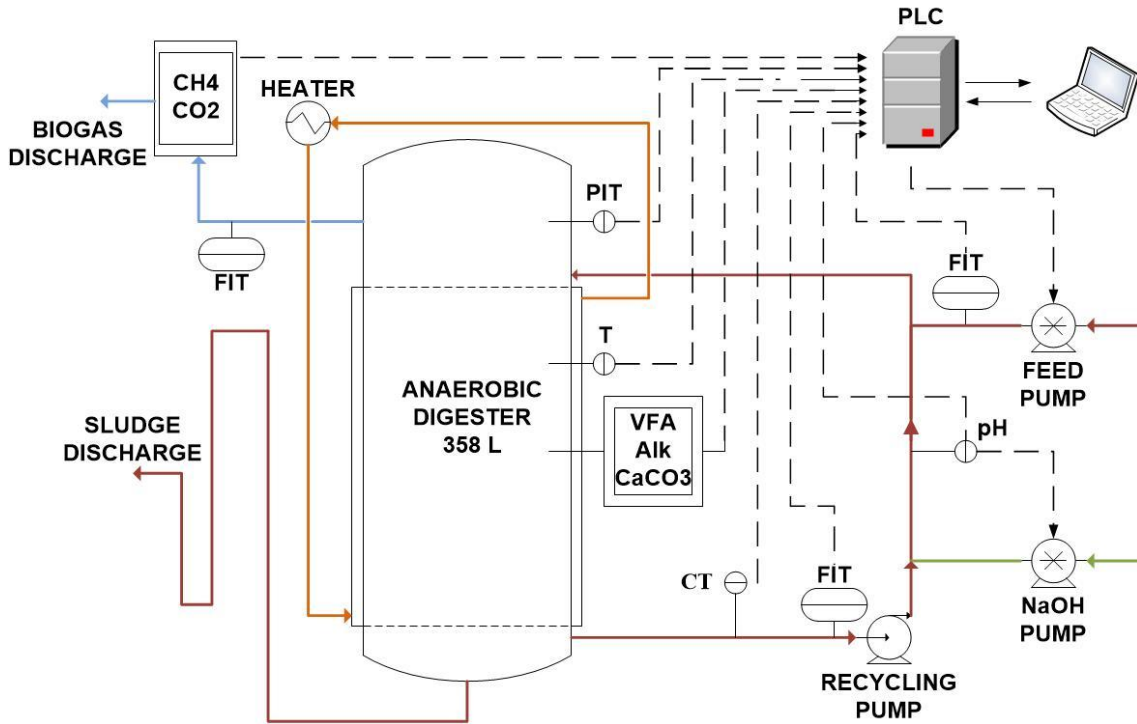
617 **Figure 5.** Evolution during the operational period of: (a) methane yield; and (b) fraction of
618 total COD removed and fraction of COD removed for methane production. (I), (II) and (III)
619 stand for the different sections of the operational period

620 **Figure 6.** Control system performance. Evolution of: (a) methane flow and influent flow; and
621 (b) VFA content in the effluent. SP stands for Set-points. The values marked with * represent
622 the 2h-moving averages of the measured values (every 60 min)

623

624 **Table 1.** Average raw wastewater characteristics

625 **Table 2.** Advanced fuzzy-logic controller action: grade of membership to the output linguistic
626 labels

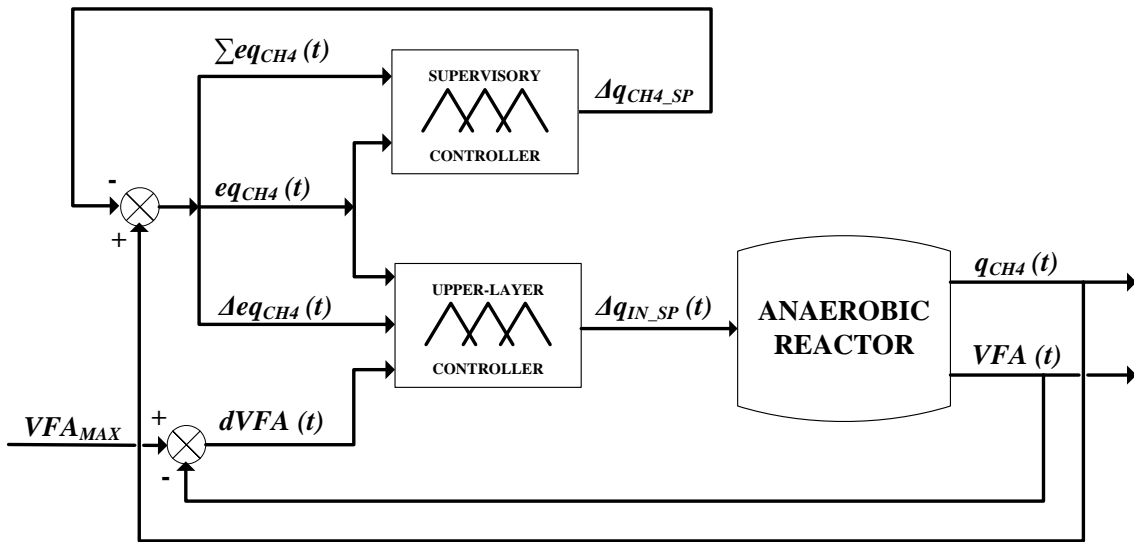


627

628 **Figure 1.** Flow diagram of the plant, including instrumentation. (Nomenclature: **FIT**: Flow-

629 Indicator-Transmitter; **PIT**: Pressure-Indicator-Transmitter; **pH**: pH-Transmitter; **CT**:

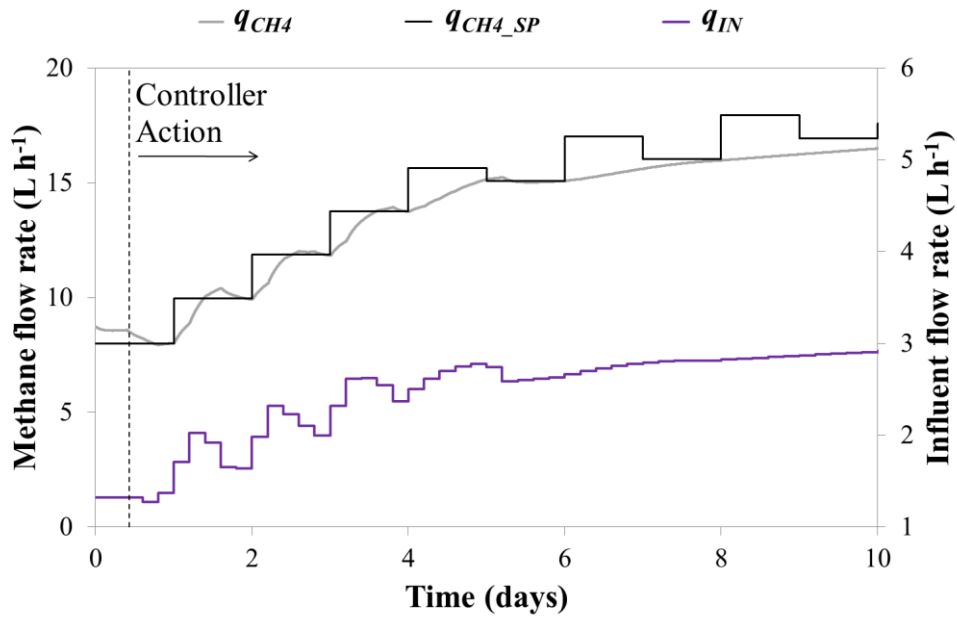
630 Conductivity-Transmitter; **T**: Temperature sensor; **PLC**: Programmable Logic Controller)



631

632

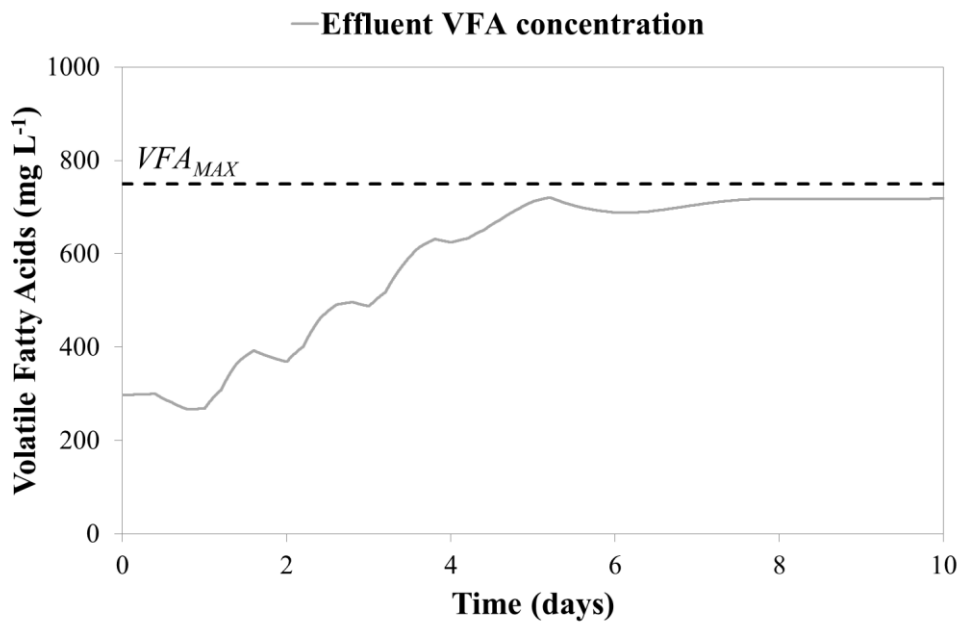
Figure 2. Flow diagram of the advanced fuzzy-logic controller



633

634

(a)



635

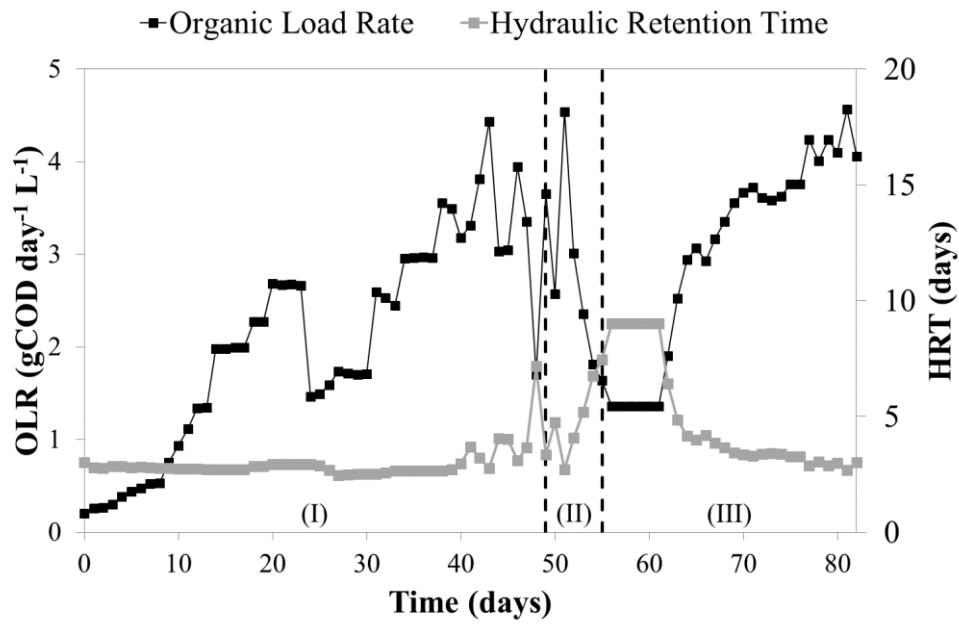
636

(b)

637 **Figure 3.** Simulation of the control system performance. Evolution of: (a) methane flow and

638

influent flow; and (b) VFA content in the effluent

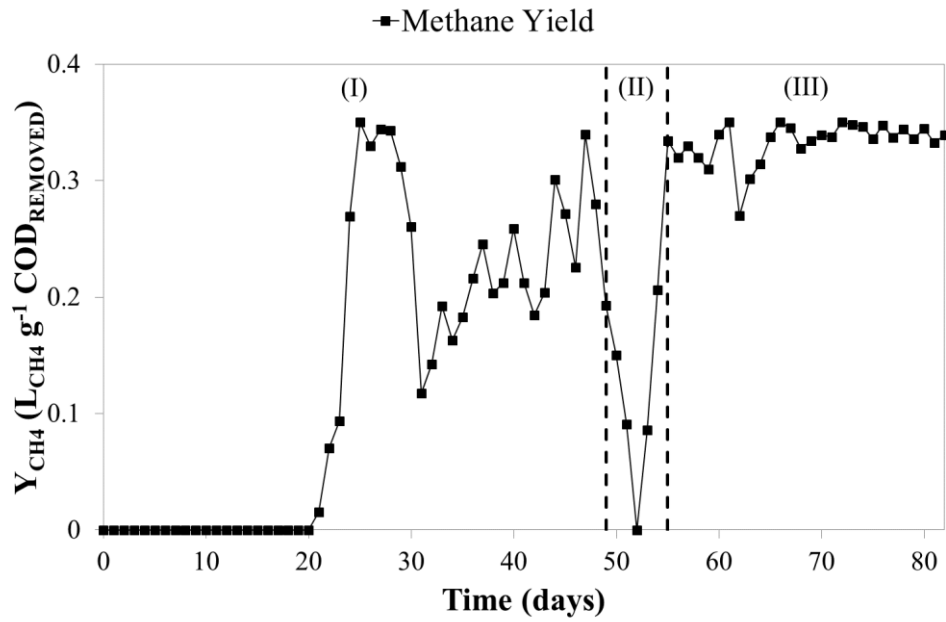


639

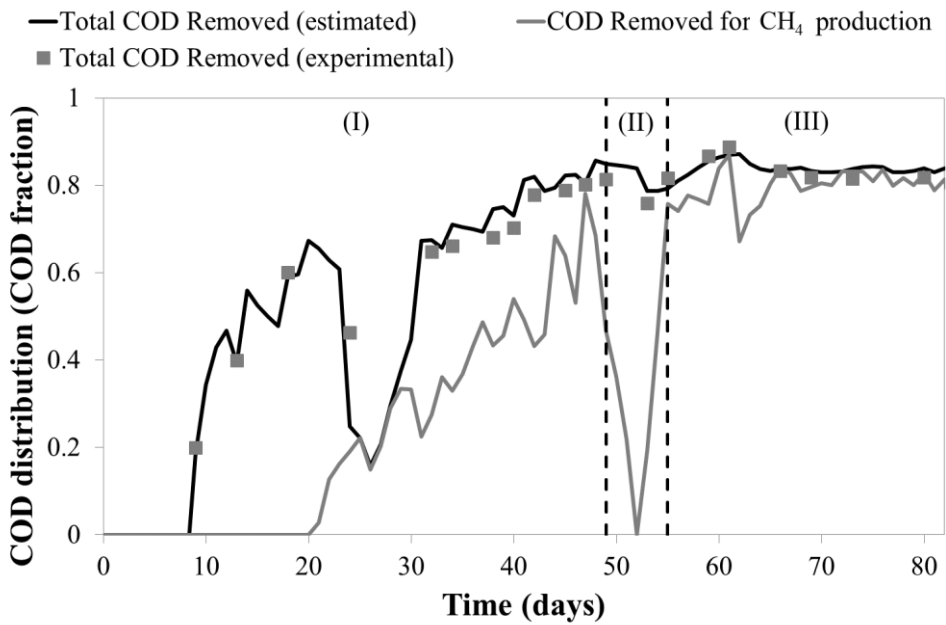
640 **Figure 4.** Evolution during the operational period of OLR and HRT. (I), (II) and (III) stand

641

for the different sections of the operational period

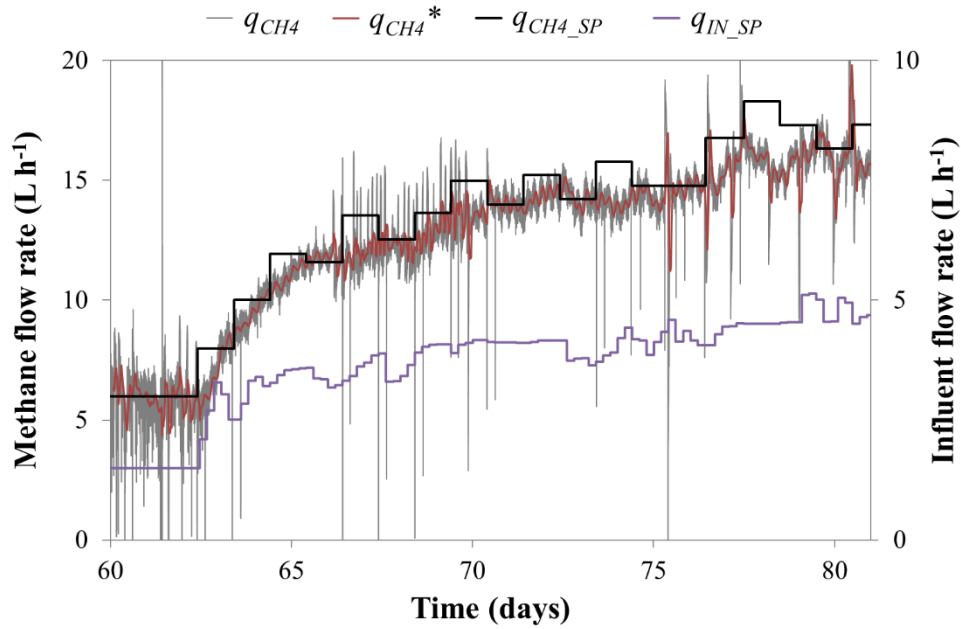


(a)



(b)

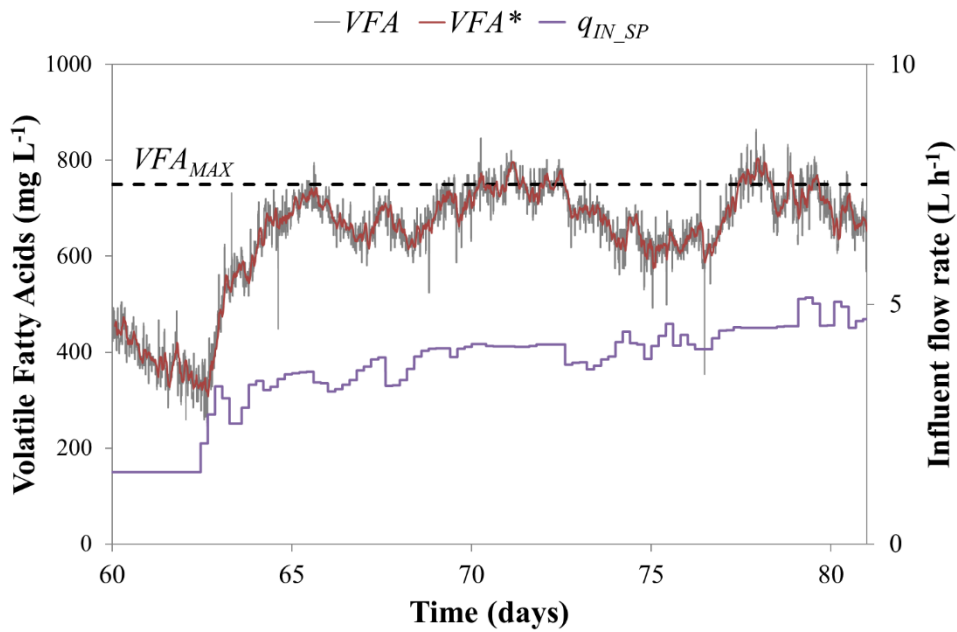
Figure 5. Evolution during the operational period of: (a) methane yield; and (b) fraction of total COD removed and fraction of COD removed for methane production. (I), (II) and (III) stand for the different sections of the operational period



649

650

(a)



651

652

(b)

653 **Figure 6.** Control system performance. Evolution of: (a) methane flow and influent flow; and

654 (b) VFA content in the effluent. SP stands for Set-points. The values marked with * represent

655 the 2h-moving averages of the measured values (every 60 min)

656 **Table 1.** Average raw wastewater characteristics

Parameter	Unit	Mean \pm SD
COD	g COD L ⁻¹	21.6 \pm 0.8
Acetate	g COD L ⁻¹	3.7 \pm 0.4
Propionate	g COD L ⁻¹	4.6 \pm 0.8
Butyrate	g COD L ⁻¹	2.8 \pm 0.3
Valerate	g COD L ⁻¹	1.5 \pm 0.7

657

658 **Table 2.** Advanced fuzzy-logic controller action: grade of membership to the output linguistic
659 labels

Inference Rule	Grade of membership to the output linguistic variables				
<i>Supervisory controller</i>					
A	$\mu (\Delta q_{CH_4_SP})_{HP}$	=	$\mu (eq_{CH_4})_Z$	·	$\mu (\Sigma eq_{CH_4})_Z$
B	$\mu (\Delta q_{CH_4_SP})_{LN}$	=	$\mu (eq_{CH_4})_N$	·	$\mu (\Sigma eq_{CH_4})_N$
C	$\mu (\Delta q_{CH_4_SP})_{LP}$	=	$\mu (eq_{CH_4})_P$	·	$\mu (\Sigma eq_{CH_4})_P$
<i>Upper-layer controller</i> * $eq_{CH_4} < 0$; ** $eq_{CH_4} > 0$					
1	$\mu (\Delta q_{IN})_{HP}$	=	$\mu (eq_{CH_4})_N$	·	$\mu (\Delta eq_{CH_4})_Z \cdot (1 - \mu (dVFA)_Z)$
2	$\mu (\Delta q_{IN})_{HP}$	=	$\mu (eq_{CH_4})_N$	·	$\mu (\Delta eq_{CH_4})_P \cdot (1 - \mu (dVFA)_Z)$
3	$\mu (\Delta q_{IN})_{HN}$	=	$\mu (eq_{CH_4})_P$	·	$\mu (\Delta eq_{CH_4})_Z$
4	$\mu (\Delta q_{IN})_{HN}$	=	$\mu (eq_{CH_4})_P$	·	$\mu (\Delta eq_{CH_4})_P$
5*	$\mu (\Delta q_{IN})_{LP}$	=	$\mu (eq_{CH_4})_Z$	·	$\mu (\Delta eq_{CH_4})_N \cdot (1 - \mu (dVFA)_Z)$
5**	$\mu (\Delta q_{IN})_{LN}$	=	$\mu (eq_{CH_4})_Z$	·	$\mu (\Delta eq_{CH_4})_N$
6*	$\mu (\Delta q_{IN})_{LP}$	=	$\mu (eq_{CH_4})_Z$	·	$\mu (\Delta eq_{CH_4})_P \cdot (1 - \mu (dVFA)_Z)$
6**	$\mu (\Delta q_{IN})_{LN}$	=	$\mu (eq_{CH_4})_Z$	·	$\mu (\Delta eq_{CH_4})_P$

660

661 **List of Abbreviations**

- 662 **AD** – Anaerobic Digestion
663 **AnMBR** – Anaerobic Membrane Bioreactor
664 **CT** – Conductivity-Transmitter
665 **EGSB** – Expanded Granular Sludge Blanket
666 **FIT** – Flow-Indicator-Transmitter
667 **GC** – Gas Chromatograph
668 **HN** – High Negative
669 **HP** – High Positive
670 **HRT** – Hydraulic Retention Time
671 **LN** – Low Negative
672 **LP** – Low Positive
673 **N** – Negative
674 **OLR** – Organic Loading Rate
675 **P** – Positive
676 **PID** – Proportional-Integral-Derivative
677 **PIT** – Pressure-Indicator-Transmitter
678 **PLC** – Programmable Logic Controller
679 **SRT** – Solid Retention Time
680 **SR** – Sampling Time
681 **T** – Temperature Sensor
682 **UASB** – Up-flow Anaerobic Sludge Blanket
683 **VFA** – Volatile Fatty Acid
684 **Z** – Zero
685

686 **List of Symbols**

- 687 q_{CH_4} – Methane flow rate
688 $G_{CORRECTED}$ – Corrected biogas flow
689 $G_{MEASURED}$ – Measured biogas flow
690 $frho$ – Volumetric correction factor
691 ρ_{AIR} – Volumetric weight of air
692 ρ_{CH_4} – Volumetric weight of CH_4
693 ρ_{CO_2} – Volumetric weight of CO_2
694 ρ_{N_2} – Volumetric weight of N_2
695 $eq_{CH_4}(t)$ – Error in methane flow rate at a given time
696 $q_{CH_4}(t)$ – Methane flow rate at a given time
697 $q_{CH_4}^*$ – 2-h moving average of $q_{CH_4}(t)$
698 $q_{CH_4_SP}$ – Set-point of methane flow rate
699 $\Delta eq_{CH_4}(t)$ – Variation in the error of the methane flow rate at a given time
700 $eq_{CH_4}(t-1)$ – Error in methane flow rate at the previous control action
701 δ – Modifying algebraic factor
702 $dVFA(t)$ – difference between VFA_{MAX} and the VFA content in the effluent at control time
703 $VFA(t)$ – Effluent VFA concentration at a given time
704 VFA^* – 2-h moving average of $VFA(t)$
705 VFA_{MAX} – Maximum effluent VFA concentration
706 $\Sigma eq_{CH_4}(t-1)$ – Accumulated error in methane flow rate at the previous control action
707 Σeq_{CH_4} – Accumulated error in methane flow rate at a given time
708 ST – Sampling time
709 p – Numerical value of a variable
710 c – Center of the Gaussian-type membership function
711 $\mu(p)$ – Degree of membership of the input variable p
712 σ – Amplitude of the Gaussian-type membership function
713 $\Delta q_{CH_4_SP}$ – Modification in methane flow rate set-point
714 q_{IN_SP} – Set-point of influent flow rate
715 Δq_{IN} – Modification of the influent flow rate
716 Y_{CH_4} – Methane yield